Hydrology and Earth System Sciences, 8(6), *1179–1185* (2004) © EGU

Hydrology & Earth System Sciences

Research Note: Derivation of temperature lapse rates in semi-arid south-eastern Arizona

R.C. Harlow[1], E.J. Burke[1], R.L. Scott[2], W.J. Shuttleworth[3], C.M. Brown[3] and J.R. Petti[3]

[1]Met Office, FitzRoy Road, Exeter, EX1 3PB, United Kingdom
[2]Southwest Watershed Research Center, ARS/USDA, 2000 E. Allen Road, Tucson, AZ, USA
[3]Department of Hydrology and Water Resources, University of Arizona, Tucson, AZ, USA

Email for corresponding author: chawn.harlow@metoffice.gov.uk

Abstract

Ecological and hydrological modelling at the regional scale requires distributed information on weather variables, and temperature is important among these. In an area of basin and range topography with a wide range of elevations, such as south-eastern Arizona, measurements are usually available only at a relatively small number of locations and elevations, and temperatures elsewhere must be estimated from atmospheric lapse rate. This paper derives the lapse rates to estimate maximum, minimum and mean daily temperatures from elevation. Lapse rates were calculated using air temperatures at 2 m collected during 2002 at 18 locations across south-eastern Arizona, with elevations from 779 to 2512 m. The lapse rate predicted for the minimum temperature was lower than the mean environmental lapse rate (MELR), i.e. 6 K km^{-1}, whereas those predicted for the mean and maximum daily temperature were very similar to the MELR. Lapse rates were also derived from radiosonde data at 00 and 12 UTC (5 pm and 5 am local time, respectively). The lapse rates calculated from radiosonde data were greater than those from the 2 m measurements, presumably because the effect of the surface was less. Given temperatures measured at Tucson airport, temperatures at the other sites were predicted using the different estimates of lapse rates. The best predictions of temperatures used the locally predicted lapse rates. In the case of maximum and mean temperature, using the MELR also resulted in accurate predictions.

Keywords: near surface lapse rates, semi-arid climate, mean minimum and maximum temperatures, basin and range topography

Introduction

Hydrological and ecological models are applied increasingly to predict distributed fields over regional scales (Thornton *et al*., 1997). Consequently, there is a need to obtain reliable distributed forcing data, but measurements are usually available only at a few low altitude locations. This paper evaluates the prediction of distributed fields of 2-m (or 'screen height') air temperature, which is an important driver for such models. In a region of basin and range topography such as south-eastern Arizona, there is a wide range of elevations and land cover which affect local temperature.

Past research in the Pacific North-western US (Lookingbill and Urban, 2003) has shown that elevation is the most important factor when predicting near-surface air temperature. The usual method for extrapolating temperature observations at a nearby site over a range of elevations is to use a prescribed lapse rate (e.g. MTCLIM; Thornton *et al*., 1997) with high-resolution elevation measurements such as those available from GTOPO-30 (http://edcdaac.usgs.gov/gtopo30/gtopo30.asp) or ASTER (Yamaguchi *et al*., 1998). This paper evaluates different estimates of lapse rates to extrapolate mean, minimum and maximum 2-m air temperature, specifically (a) the mean environmental lapse rate (MELR; assumed to be 6 K km^{-1}); (b) the lapse rate derived from a network of near-surface meteorological stations; and (c) the lapse rate derived from radiosonde profiles.

Data and Methods

SURFACE METEOROLOGICAL STATIONS

The study area for this investigation is south-eastern Arizona (Fig. 1). The surface observation sites (Table 1) are distributed across the region with a range of aspects, land cover and elevation. Elevations of the sites range from 779 m to 2900 m. Seven of the sites are riparian, three are forested, four are rangeland and three lie within urban areas. The data from the site at Mount Bigelow are in fact the averaged value for three sites within 2 km of each other and separated by less than 100 m in the vertical. Data were collected at a frequency of between 15 and 60 minutes at all these surface sites and the minimum, maximum and mean temperatures were selected and/or calculated from these time series of observations.

UPPER AIR DATA

Upper air data were available every day at 0000 and 1200 UTC (i.e. 5 pm and 5 am, local time, respectively). The data analysed here were collected using radiosondes launched from Tucson International Airport (32.117° N, 110.93° W).

LAPSE RATE ESTIMATION

Lapse rates are the rate of change of temperature with height, i.e.

$$T = T_0 - \Gamma.dz \qquad (1)$$

where T_0 is the temperature at the base location, T is the temperature at a second location, Γ is the lapse rate, and dz is the difference in elevation between the two locations. Lapse rates for mean ($L_{mean,sur}$), minimum ($L_{min,sur}$) and maximum ($L_{max,sur}$) daily temperatures were calculated using a time series of ten-day running means of the observed screen-height temperatures to average out short-term effects such as the passage of fronts or convective storms. The lapse rates and estimated errors therein were estimated for each day using a linear regression between the 10-day running mean temperature and elevation. Similarly, lapse rates for the 0Z ($L_{max,air}$) and 12Z ($L_{min,air}$) radiosonde data were

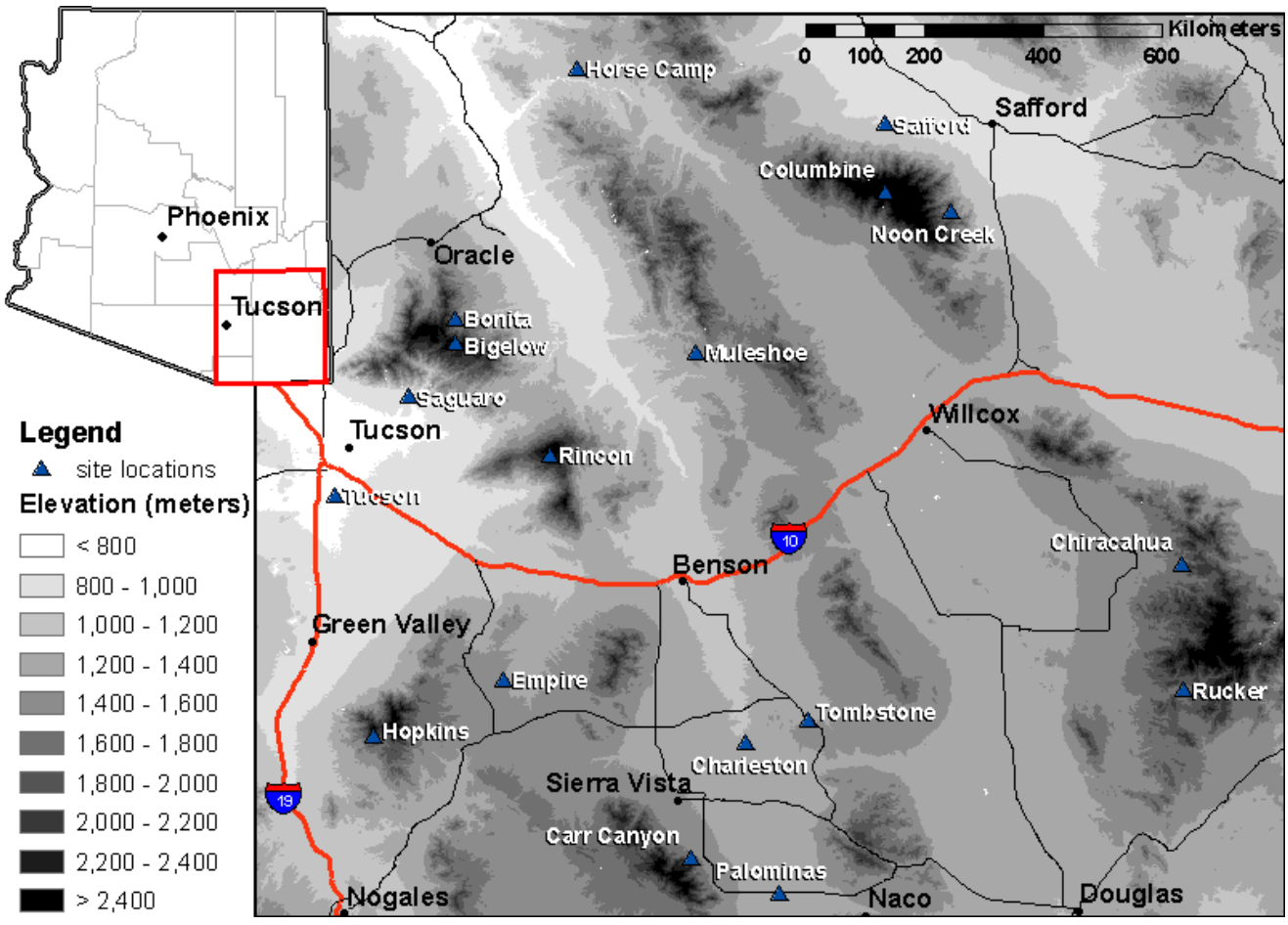

Fig. 1. *Map of site locations with shaded elevation contours. Expanded study area map shows individual site locations on shaded relief.*

calculated using a linear regression between the ten-day running mean of temperature (linearly interpolated to altitudes equivalent to those of the surface stations) and elevation.

Results

Daily mean, minimum and maximum temperatures were calculated for each of the eighteen observation sites listed in Table 1. Figure 2 shows (in black) ten-day mean values of the mean, minimum and maximum observed surface air temperatures as a function of elevation, with the mean centred around day of the year (DOY) 90, 180, 270 and 360. The symbols denote the measurement sites. As expected, the profiles show (with some local discrepancies) a general decrease in temperature with increasing elevation. Also shown (in grey) are ten-day mean values of the radiosonde air temperature observation at 00 UTC (approximately the time of maximum temperature) and 12 UTC (approximately the time of minimum temperature). For consistency, the radiosonde data were interpolated linearly to the heights of surface stations (represented by the symbols). The radiosonde data show a smoother decrease in temperature with increasing elevation than the surface station data. This is presumably because the radiosondes ascend from a single location and, once airborne, the surface has minimal impact on observations. The surface observations are, on the other hand, scattered over south-eastern Arizona and over a range of land cover types, slopes and aspects; consequently, they exhibit significantly greater variability. At 12 UTC (near minimum temperature), there is some decrease in temperature towards the surfacee due to nocturnal radiative cooling. The diurnal variation in the surface measurements is slightly greater than that in the radiosonde measurements, particularly at the higher elevations, presumably because surface radiative heating by day and cooling at night has less effect on air temperature further from the ground.

Figure 3 shows the time series of lapse rates calculated using the surface observations for the mean ($L_{mean,sur}$), minimum ($L_{min,sur}$) and maximum ($L_{max,sur}$) observed air temperature by fitting a linear regression model of ten-day running mean temperature as a function of elevation. The error bars represent the 95% confidence intervals of the linear regression. The MELR (6 K km^{-1}) is shown as a bold gray line. $L_{max,sur}$ is generally slightly greater than the MELR whereas $L_{min,sur}$ is noticeably less than the MELR (see also Table 2). The mean daily temperature has a mean annual lapse rate approximately equal to the MELR (Table 2). There is a distinct annual variation in the estimated lapse rates. For example, in the colder season, when the mean daily temperature at 779 m (Tucson) is generally less than 10 °C, $L_{mean,sur}$ is lower then the MELR, whereas in the warmer season when the temperature is generally greater than 30 °C $L_{mean,sur}$ is greater than the MELR. $L_{max,sur}$ has the smallest intra-annual variability and $L_{min,sur}$ the greatest, although this is more a result of noticeable differences in the day-to-day values, rather than of an overall increase in the annual signal.

Table 1. List of sites included in present study, including a short description and their elevation.

Site name	*Elevation (m)*	*Latitude (°N)*	*Longitude (°W)*	*Description*	*Agency*
Bigelow	2400	32:25:00	110:43:32	Forested hilltops (2) and convex S-facing slope	SAHRA
Bonita	1346	32.27.36	109.55:48	Agricultural	AZMet
Carr Canyon	1646	31:26:42	110:16:48	North-eastern facing riparian	RAWS
Chiracahua	1646	32:00:00	109:21:00	Western facing riparian	RAWS
Columbine	2902	32:42:14	109:54:50	Forest with neutral slope	RAWS
Empire	1417	31:46:50	110:38:05	Rangeland	RAWS
Hopkins	2170	31:40:31	110:52:48	Mountain top	RAWS
Horse Camp	1231	32:56:15	110:29:46	Riparian	RAWS
Muleshoe	1273	32:24:00	110:16:15	Rangeland (?)	RAWS
Noon Creek	1501	32:40:04	109:47:17	Eastern facing riparian	RAWS
Palominas	1290			Riparian	ARS
Rincon	2512	32:12:20	110:32:53	Forest	RAWS
Rucker	1737	31:45:40	109:20:55	Western facing riparian	RAWS
Riparian	1212				ARS
Safford	901	32:50:00	109:43:00	Agricultural	AZMet
Saguaro	945	32:19:00	110:48:48	Rangeland	RAWS
Tombstone	1390	31.42:36	110.03:36	Rangeland	ARS
Tucson	779	32.07:52	110.24:20	Metropolitan	AZMet

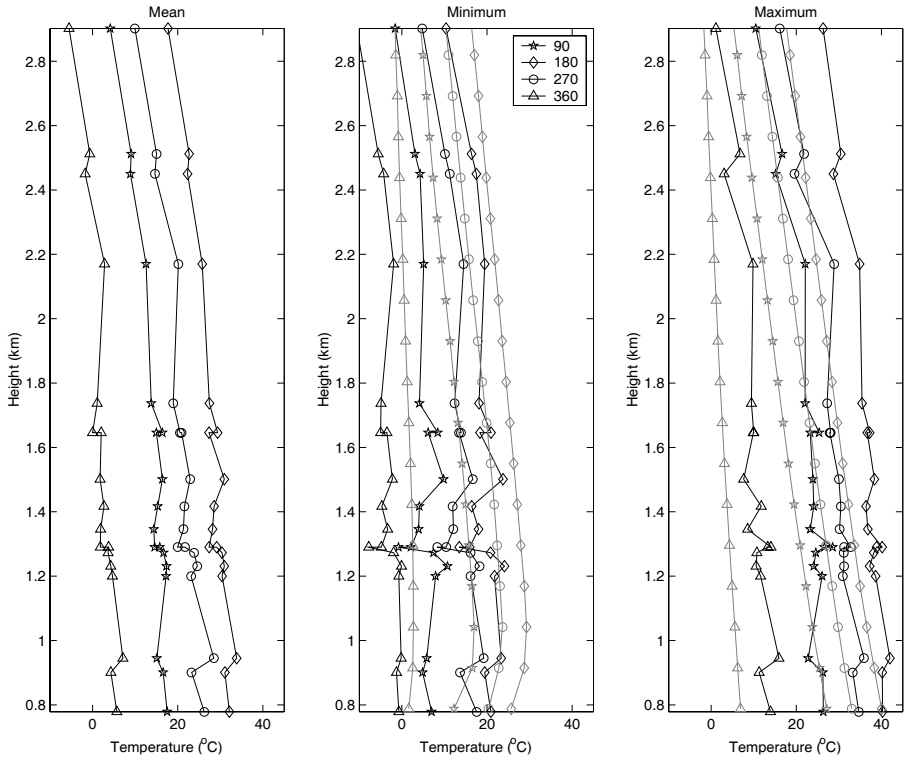

Fig. 2. *The time series of lapse rates calculated using the surface observations for the mean, minimum and maximum observed air temperature. The error bars represent the 95% confidence intervals of the linear regression. Also shown (in grey) is the MELR.*

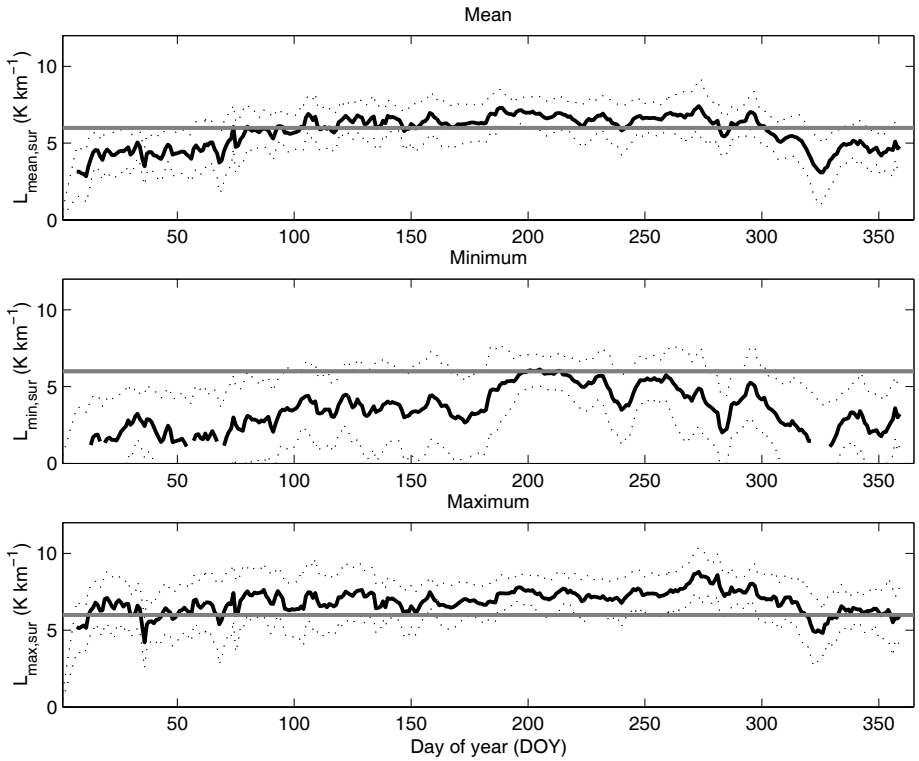

Fig. 3. *Profiles of ten-day mean values of the mean, minimum, and maximum observed surface air temperatures (black) and the 00Z and 12Z radiosonde measurements (grey) as a function of elevation with the means centered around day of the year (DOY) 90, 180, 270, and 360. The symbols represent the measurement sites in Table 1.*

Table 2. Estimated mean lapse rates for the surface micrometeorological measurements and the radiosonde measurements.

	Surface lapse rates (K km^{-1})			Radiosonde lapse rates (K km^{-1})	
	$L_{mean,sur}$	$L_{\min,sur}$	$L_{\max,sur}$	$L_{\min,air}$	$L_{\max,air}$
Annual mean	5.732	3.563	6.844	6.2873	8.9641
Standard deviation of mean	1.0575	1.3181	0.7276	1.39	1.72
Uncertainty	0.65	1.16	0.74	0.095	0.108

Table 2 also gives a measure of the intrinsic uncertainty in the measurements, which is taken as the quarter-width of the confidence interval in the regression. The uncertainty in these estimates of lapse rates is less than the intra-annual variability, as represented by the standard deviation of the mean. Errors in the calculated surface lapse rates are greatest for the minimum temperature, perhaps because of local canopy and cloud conditions and topographic siting. Nocturnal radiative cooling depends on cloud cover, differences in wind shelter between open and forested areas (Karlson, 2000), local cold air advection in forested areas (Mahrt *et al.*, 2000), and cold air drainage, such as that observed by Mahrt *et al.* (2001) and Soler *et al.* (2002) in a wide, shallow gulley. These mechanisms will all cause local differences in near-surface air temperature, greater scatter in the regression of temperature against height and, thus, greater error in the calculated lapse rate. The variability in such influences from night to night also leads to greater standard deviation in the means.

Figure 4 shows the daily lapse rate calculated using the ten-day running mean of radiosonde temperature data assuming a linear variation with height, with the error bars again representing the 95% confidence intervals. (Note: the lowest levels in the 12Z data are neglected because of the temperature inversion near the surface). The MELR is also shown in Fig. 4. The lapse rates for both 0Z ($L_{min,air}$) and 12Z ($L_{max,air}$) are greater by 2–3 K km^{-1} than their counterparts obtained from the surface data. Hence, the mean value of $L_{min,air}$ is approximately equal to the MELR whereas that of $L_{max,air}$ is significantly greater. Also, the intrinsic uncertainty in the estimated lapse rates (represented by the error bars) is significantly smaller than for the surface measurements (see also Table 2). However, the intra-annual variation in the lapse rates deduced from radiosonde observations is similar to that for surface observations. There is again an increase in the lapse rates in summer when temperatures are higher and a decrease in the cooler winter months.

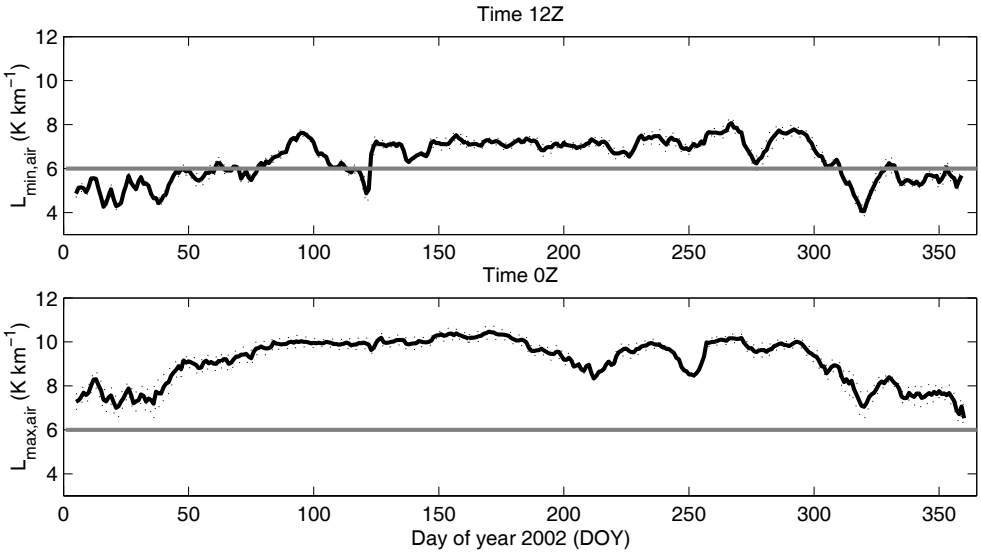

Fig. 4. *The time series of lapse rates calculated using the radiosonde for the minimum and maximum observed air temperature. The error bars represent the 95% confidence intervals of the linear regression. Also shown (in grey) is the MELR.*

EVALUATION OF THE ESTIMATED LAPSE RATES

The different lapse rates were evaluated by predicting the mean, minimum and maximum temperatures at the different surface measurement sites. The Tucson site was taken as the base site (T_0 in Eqn. 1). Tucson has very long-term temperature records and is the location from which the radiosondes are launched. The ability to estimate the measured temperatures at all of the other surface measurement sites was then quantified. To make the verification data set independent, the lapse rates used in the extrapolation ($L_{mean,sur}$, $L_{min,sur}$ and $L_{max,sur}$) were recalculated excluding the data from the verification site under consideration in each case. Figure 5 shows the mean profile of the root mean square error between estimated and measured temperatures at the surface stations. The values marked 'meas' in Fig. 5 use the lapse rates from the surface measurements as depicted in Fig. 3. Those marked 'sound' use lapse rates from the radiosonde measurements as shown in Fig. 4. Finally, those marked '6' use a constant lapse rate of 6 K km^{-1}. On average, the error between measured and modelled temperatures is 5 °C; the error is smallest for the mean daily temperature and largest for the minimum temperature. In all cases, the lapse rates calculated from the surface measurements result in predictions with the smallest error. For the mean and maximum temperature, the MELR predicts temperatures similar to those predicted by the lapse

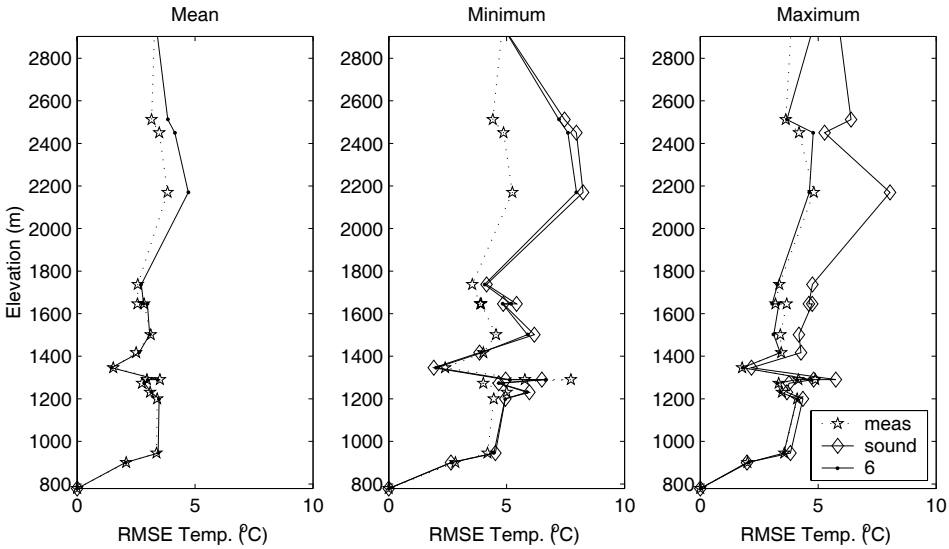

Fig. 5. *The mean annual profile of the root mean square error between estimated and measured surface stations calculated using the MELR, the surface measurements of temperature and the radiosonde measurements of temperature.*

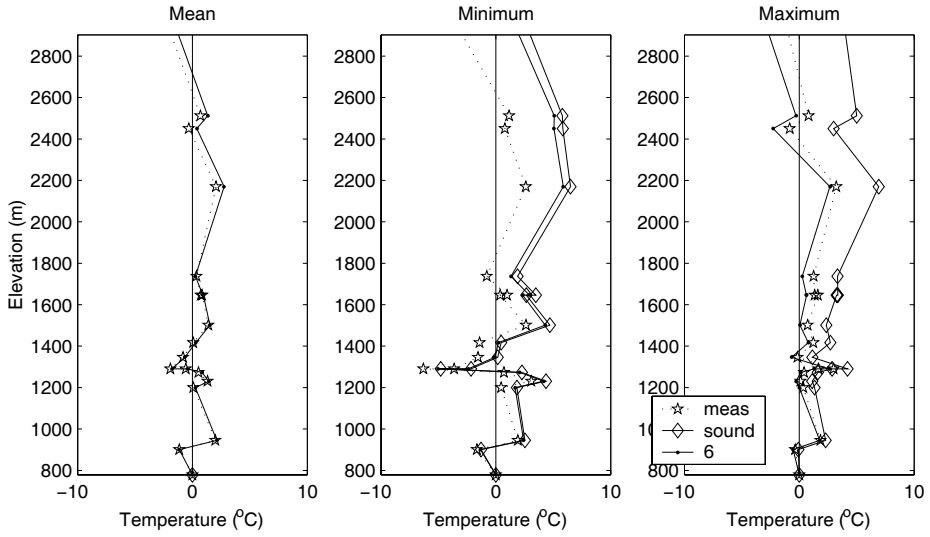

Fig. 6. *The mean annual profile of the bias between estimated and measured surface stations calculated using the MELR, the surface measurements of temperature and the radiosonde measurements of temperature.*

rates from the surface measurements. However, in the case of the minimum temperature, there is a significant disadvantage in using the MELR. Figure 6 shows a profile of the mean bias between the measured and predicted surface temperatures. Again the predictions using $L_{mean,sur}$, $L_{min,sur}$ and $L_{max,sur}$ yield the smallest bias and the MELR produces good agreement with measurements. However, the use of $L_{min,air}$, and $L_{max,air}$ results in a bias that increases with increasing separation from the base station (at 779 m).

Discussion and conclusions

The lapse rates estimated from the surface temperatures are approximately equal to the MELR for the mean temperature, lower for the minimum temperature, and greater for the maximum temperature. Thornton *et al*. (1997) carried out a study of temperature lapse rates over the Pacific North-west. This region differs from that studied here in that it has a temperate climate and it covers a larger area with a greater range in elevation. Nonetheless, the annual time-series of lapse rates found in the two studies are broadly comparable. In this study, the errors on the predicted lapse rate for the minimum temperature are greater than those for the maximum and mean. This is because the stable atmosphere at night is reinforced by cold air drainage which depends on location. There is an intra-annual variation in the estimated lapse rates that is greater than the error in each individual estimate of lapse rate, with the lapse rates on average being greater in summer and less in winter. The lapse rates calculated from the radiosonde data have a much smaller estimated error, perhaps because they are less susceptible to near-surface effects. The lapse rates calculated from the radiosonde data do, however, show a similar intra-annual variation to those calculated from surface data. On average, the errors in the estimated temperature are of the order of 5 K. As might be expected, the lapse rates derived from the surface measurements provided the best estimates of temperature. However, in the case of the mean and maximum daily temperature, the MELR produces similar errors.

The implications of these results for deriving temperature for forcing surface models in semi-arid regions such as the study area are two-fold. For modelling near-surface processes that depend most strongly on mean and maximum temperatures, such as snowmelt and evapotranspiration, the MELR can be used with adequate accuracy. For those processes that are strongly affected by minimum temperature, such as growing season length (determined by frost-free days), or those that depend on diurnal temperature range, neither the MELR nor the radiosonde data give lapse rates as low as those actually observed by the surface network. For this semi-arid region, the average lapse rate for minimum temperature was found to be 59% of the MELR and 54% of the lapse rate calculated from radiosonde data.

Acknowledgements

Primary funding for the research presented in this paper was provided from the National Science Foundation's Science and Technology Center (STC) program through the Center for Sustainability of semi-Arid Hydrology and Riparian Areas (SAHRA) under Agreement EAR-9876800. Eleanor Burke was funded under NOAA project NA16GP2002. The data used in this study were provided by SAHRA, the Tucson ARS/USDA, and the Western Regional Climate Center's Remote Automated Weather Station program.

References

Karlsson, I.M., 2000. Nocturnal air temperature variations between forest and open areas. *J. Appl. Meteorol.,* **39,** 851–862.

Lookingbill, T.R. and Urban, D.L., 2003. Spatial estimation of air temperature differences for landscape-scale studies in montane environments. *Agr. Forest Meteorol.,* **114,** 141–151.

Mahrt, L., Lee, X.H., Black, A., Neumann, H. and Staebler, R. M., 2000. Nocturnal mixing in a forest subcanopy. *Agr. Forest Meteorol.,* **101,** 67–78.

Mahrt, L., Vickers, D., Nakamura, R., Soler, M.R., Sun, J.L., Burns, S. and Lenschow, D.H., 2001. Shallow drainage flows. *Bound.-Lay. Meteorol.,* **101,** 243–260.

Soler, M.R., Infante, C., Buenestado, P., and Mahrt, L., 2002. Observations of nocturnal drainage flow in a shallow gully. *Bound.-Lay. Meteorol.,* **105,** 253–273.

Thornton, P.E., Running, S.W. and White, M.A., 1997. Generating surfaces of daily meteorological variables over large regions of complex terrain. *J . Hydrol.,* **190,** 214–251.

Yamaguchi, Y., Kahle, A., Tsu, H., Kawakami, T. and Pniel, M., 1998. Overview of Advanced Space-borne Thermal Emission and Reflection Radiometer (ASTER). *IEEE Trans. Geosci. Remot. Sen.,* **36,** 1282–1289.